



Cite this: *Nanoscale Adv.*, 2025, 7, 6265

Received 26th April 2025  
Accepted 28th July 2025

DOI: 10.1039/d5na00405e  
[rsc.li/nanoscale-advances](http://rsc.li/nanoscale-advances)

## Preserving enzyme conformation and catalytic efficiency in crowded and active environments

Arnab Maiti, Nividha and Krishna Kanti Dey \*

Proteins operate in dynamic environments where interactions and fluctuations influence their structure and function. Understanding how these factors contribute to enzyme stability is essential for both fundamental biology and practical applications. Here, we investigate the role of protein–protein interactions and non-thermal active fluctuations in enzyme conformational dynamics and catalytic activity. Our findings reveal that in a dense suspension, enzyme catalytic activity and structural integrity are preserved for extended periods. Additionally, we observed that mechanical fluctuations generated by enzyme catalytic reactions help sustain enzymatic activity over longer timescales.

## Introduction

Enzymes have long been of research interest due to their exceptional catalytic efficiency, substrate specificity, biodegradability, and sustainability. Their ability to operate under mild conditions, produce high-purity products, and minimize environmental impact makes them essential elements in various industrial and biomedical applications. However, despite these advantages, working with enzymes often involves several challenges, including high production and purification costs, limited stability in harsh or non-native environments, and susceptibility to inhibition at elevated substrate or product concentrations. From an industrial perspective, optimizing enzyme stability, processing efficiency, and cost-effectiveness while ensuring non-toxicity and environmental sustainability is crucial. Current enzyme development primarily focuses on protein engineering,<sup>1–3</sup> while chemical additives and physico-chemical modifications offer cost-effective strategies to enhance stability and catalytic efficiency.<sup>4,5</sup>

Beyond industrial applications, fundamental studies on protein mobility and conformational dynamics are crucial for understanding enzyme function in both *in vitro* and *in vivo* environments. While most *in vitro* biochemical studies are conducted in dilute solutions, the cellular environment is highly crowded, with up to 30–40% of the cytosol occupied by macromolecules such as proteins, polysaccharides, and nucleic acids.<sup>6</sup> Studies indicate that macromolecular crowding significantly influences protein folding, mobility, and enzymatic activity,<sup>7</sup> often enhancing stability by restricting the entropy of unfolded states and protein crowder interactions.<sup>8,9</sup> However, the effects of crowding on enzyme catalysis remain complex,

with reports of enhanced reaction rates, loss of activity, or negligible changes depending on specific conditions.<sup>5,10–13</sup> Notably, enzymes naturally accumulate at high concentrations within cells in response to environmental stress, enabling organisms to endure harsh conditions without disrupting key physiological processes such as metabolism.<sup>14</sup> At such concentrations, enzyme structures may undergo compaction, leading to suppressed conformational fluctuations. This structural compaction, combined with the crowded cellular environment, can influence enzyme stability and activity, potentially modulating their catalytic efficiency under varying conditions.

Here, we investigate the influence of protein–protein interactions and non-thermal active fluctuations on enzyme conformational dynamics and catalytic activity. Understanding how enzymes maintain their stability and efficiency under complex crowded environment is essential for both fundamental research and industrial applications. Our findings reveal that in dense suspensions, enzymes retain their structural integrity and catalytic function over extended periods. Furthermore, we demonstrate that fluctuations arising from enzyme catalytic reactions play a key role in sustaining enzymatic activity (Fig. 1). Building on existing theories of entropy-mediated enzyme stabilization and the effects of self-propulsion of catalytic motors on their environment at low Reynolds number conditions, we propose possible mechanisms to explain and validate our experimental observations.

## Results and discussion

It has already been reported that the denaturation and therefore the catalytic efficiency of enzymes diminishes over time in aqueous solutions due to their enhanced conformational entropy in the unfolded state.<sup>15</sup> In this study, we focus on catalase and urease, two extensively studied enzymes known for their robustness, high turnover rates, and ability to generate

Laboratory of Soft and Living Materials, Department of Physics, Indian Institute of Technology Gandhinagar, Palaj, Gandhinagar, Gujarat 382055, India. E-mail: [kdey@iitgn.ac.in](mailto:kdey@iitgn.ac.in)



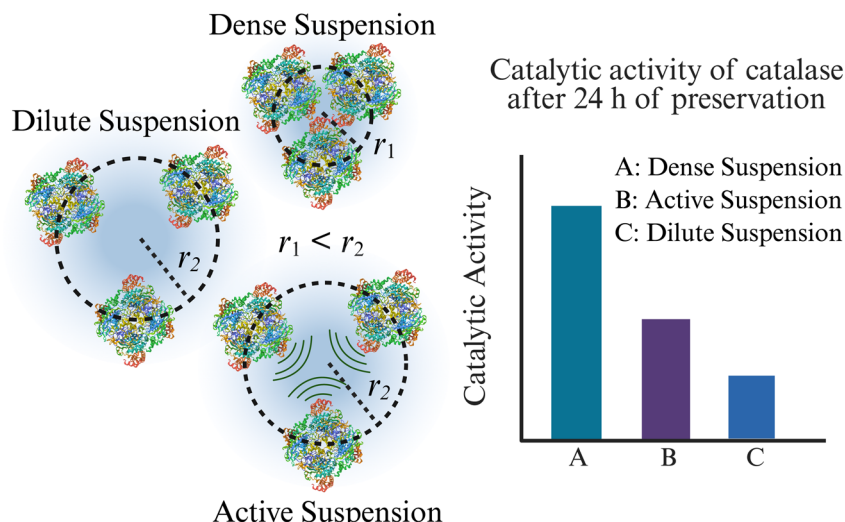


Fig. 1 Catalytic activity of catalase was assessed after 24 h of preservation in three different stock solutions: dilute catalase suspension, dense catalase suspension, and active catalase suspension. In the dense suspension, reduced intermolecular distance promotes greater protein–protein interaction and enhanced stability. In the active suspension, enzyme molecules generate mechanical fluctuations during substrate turnover, which also help sustain their stability and catalytic activity over longer periods.

significant active mechanical fluctuations during catalysis.<sup>16–19</sup> These enzymes have been reported to influence the behaviour of nearby molecules during catalysis, which may have important implications in maintaining enzyme stability under dense conditions. To assess the functional stability of catalase under different crowding conditions, three stock solutions with concentrations of 1 nM, 1  $\mu$ M, and 10  $\mu$ M were prepared and stored at 23 °C. At 24 h intervals, the decomposition rate of 10 mM H<sub>2</sub>O<sub>2</sub> was measured using 1 nM enzyme prepared from each stock solution. Enzyme activity was quantified by monitoring the change in absorbance over an initial 120 s period, normalized to the reaction rate of a freshly prepared sample (0 h). Fig. 2(a) shows the decomposition kinetics for the three stock solutions after 48 h. The highest reaction rate was observed for enzymes from the 10  $\mu$ M stock solution, while the lowest was from the 1 nM stock solution. Fig. 2(b) presents the time-dependent activity of enzymes from different stock solutions, revealing a clear trend: enzyme activity declines over time, with the rate of decline dependent on stock solution concentration. Notably, enzymes in higher-concentration suspensions

retained catalytic activity for a significantly longer duration compared to those in dilute solutions.

Since protein functionality is closely linked to its conformation,<sup>20</sup> we further examined structural stability using fluorescence spectroscopy. In solution, thermal energy causes solvent molecules to bombard the protein surface randomly, leading to structural unfolding.<sup>21,22</sup> Both catalase and urease contain aromatic amino acids such as tryptophan and tyrosine, whose fluorescence properties serve as indicators of structural integrity. The intrinsic fluorescence of catalase, with an excitation at 280 nm and emission at 336 nm, diminishes upon structural perturbation. Fig. 3(a) and (b) depict the fluorescence intensity decay over time for catalase stock solutions of 300 nM and 10  $\mu$ M respectively, while Fig. 3(c) compares the time-dependent fluorescence intensity for both concentrations. The results clearly show that in dilute solutions, fluorescence intensity declines more rapidly, indicating faster conformational changes. In contrast, dense suspensions provide greater structural stability, minimizing conformational fluctuations and preserving enzymatic integrity over time.

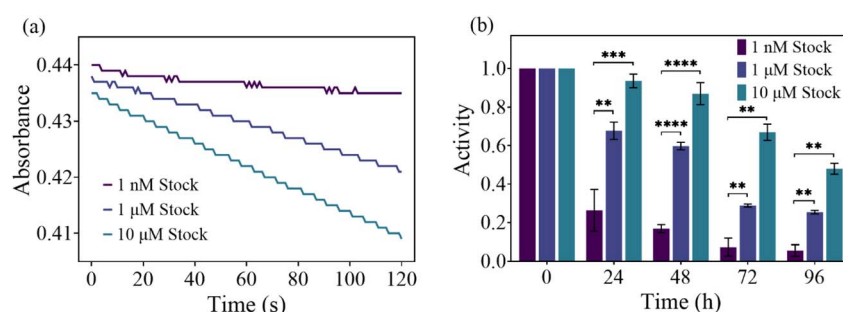


Fig. 2 (a) Decomposition kinetics of 10 mM H<sub>2</sub>O<sub>2</sub> in the presence of 1 nM catalase, taken from three stock solutions (1 nM, 1  $\mu$ M, and 10  $\mu$ M) after 48 h of storage. (b) Time-dependent decrease in catalase catalytic activity for the same stock solutions for a period of 96 h. Data were normalized with respect to the catalytic activity measured at time  $t = 0$  h.



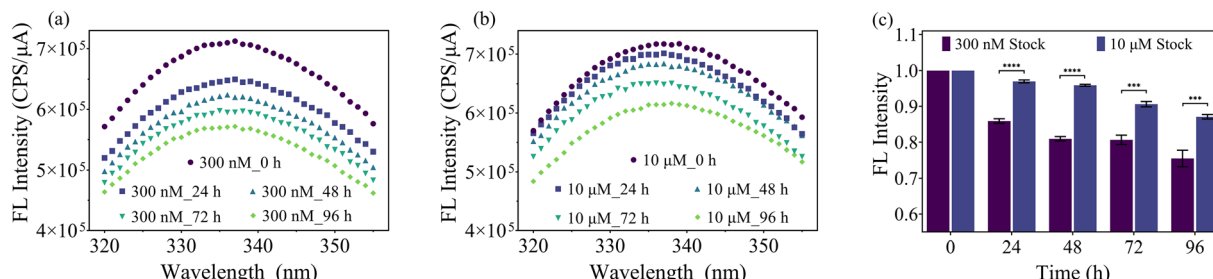


Fig. 3 Fluorescence emission spectra of 300 nM catalase from two different stock solutions ((a) 300 nM (b) 10  $\mu$ M) measured at varying storage times. (c) Time-dependent fluorescence intensity decay of 300 nM catalase, taken from stock solutions of 300 nM and 10  $\mu$ M. Data were normalized with respect to the fluorescence intensity measured at time  $t = 0$  h.

The fluorescence measurements clearly indicate time-dependent changes in enzyme conformation, leading to a gradual decline in their catalytic efficiency. Importantly, protein conformation is typically represented by its secondary structure, which exhibits characteristic spectral features in the range of 190 to 250 nm, usually characterized by the circular dichroism (CD) spectroscopy. In the CD spectra, a minimum at 208 nm corresponds to  $\alpha$ -helix absorption, while a minimum at 215 nm represents  $\beta$ -sheet absorption. To assess conformational stability, CD spectra of 300 nM catalase were obtained from two different stock solutions (300 nM and 10  $\mu$ M) and are shown in Fig. 4(a) and (b). The  $\alpha$ -helix content, calculated from the CD spectra,<sup>20,23</sup> is presented in Fig. 4(c). The results indicate that  $\alpha$ -helical content is higher in dense suspensions compared to the dilute ones, confirming enhanced structural stability in concentrated enzyme solutions.

This raises an important question: Why does enzyme activity decline at different rates despite identical physical and chemical conditions across stock solutions? The key difference between dilute and dense suspensions lies in protein number density. In denser solutions, the intermolecular distance is reduced, leading to stronger intermolecular interactions. One possible explanation is excluded volume repulsion, where proteins experience physical hindrance due to close packing, favouring the folded state of the proteins. If excluded volume effects were the dominant stabilizing factor, the presence of other macromolecules would also enhance the stability. To test

this hypothesis, we measured the catalytic activity of 1 nM catalase in the presence of 10 mM  $\text{H}_2\text{O}_2$ , under different crowding conditions using both artificial crowders (Glycerol, Ficoll 70, Ficoll 400, Dextran 70) and biological crowders (Urease enzyme and BSA). Catalase (250 kDa) has an estimated hydrodynamic radius of 5.2 nm,<sup>24</sup> which is comparable to that of Ficoll 70 (70 kDa,  $R_h \approx 4.06$  nm<sup>25</sup>), Ficoll 400 (400 kDa,  $R_h \approx 7.26$  nm<sup>25</sup>), Dextran 70 (70 kDa,  $R_h \approx 6.49$  nm<sup>26</sup>), Urease (544 kDa,  $R_h \approx 7$  nm<sup>27</sup>), and BSA (66.43 kDa,  $R_h \approx 3.5$  nm<sup>28</sup>). Glycerol, in contrast, is a small molecule (92 Da) with a negligible hydrodynamic radius ( $\sim 0.7$  nm<sup>29</sup>). Fig. 5 compares catalase activity in these crowded environments with that in deionized (DI) water. While activity decreases over time in all conditions, a mild enhancement in stability was observed in the presence of Ficoll 70 and Ficoll 400, likely due to steric interactions between these crowders and catalase.<sup>30,31</sup>

Despite the comparable size of catalase and the larger crowders, no significant stabilization of enzyme activity was observed, indicating that excluded volume effects alone cannot account for the concentration-dependent enhancement of catalase stability. These results suggest that macromolecular crowding – driven solely by steric exclusion – is not sufficient to preserve enzyme function in dense suspensions. Rather, our findings highlight the role of catalase self-interactions in maintaining structural integrity. In concentrated solutions, reduced intermolecular spacing increases the probability of transient molecular encounters, implying that stabilization

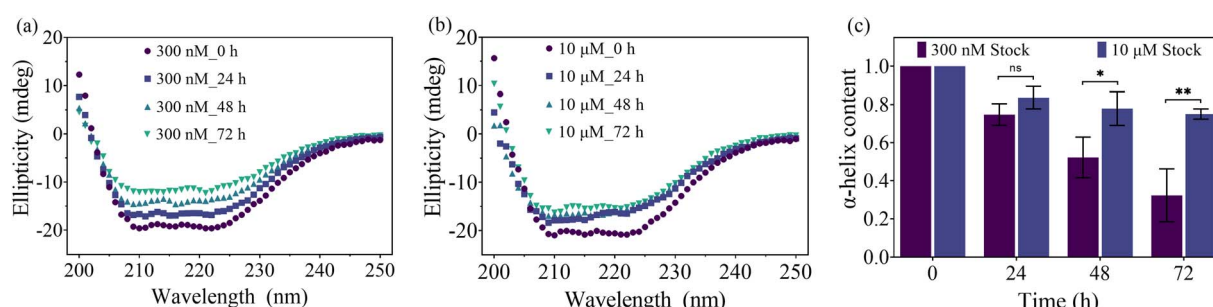


Fig. 4 CD spectra of 300 nM catalase taken from two different stock solutions: (a) 300 nM and (b) 10  $\mu$ M, recorded at different preservation times. (c) Time-dependent decay of the  $\alpha$ -helix content in 300 nM catalase taken from the two different stock solutions. Data were normalized with respect to the  $\alpha$ -helix content measured at time  $t = 0$  h.



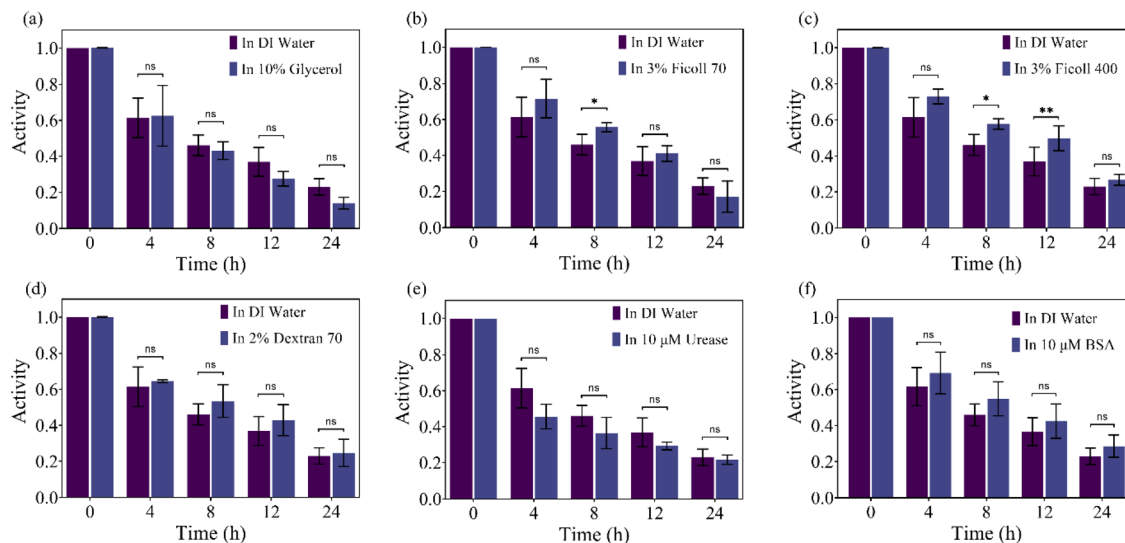


Fig. 5 Time-dependent decay of catalase activity in various crowded environments along with that in the DI water: (a) 10% Glycerol, (b) 3% Ficoll 70, (c) 3% Ficoll 400, (d) 2% Dextran 70, (e) 10  $\mu$ M Urease suspension, and (f) 10  $\mu$ M BSA suspension. Data were normalized with respect to the catalytic activity measured at time  $t = 0$  h.

arises from more than just volume exclusion. At 10  $\mu$ M catalase, the average intermolecular distance ( $\sim$ 68 nm) is only a few times larger than the molecular diameter ( $\sim$ 10 nm), allowing dynamic proximity even in the absence of stable binding. Under such conditions, weak, long-range interactions<sup>32-34</sup> are likely to modulate enzyme behaviour. Additionally, transient clustering or self-association may reduce conformational entropy and shield enzymes from denaturation, contributing to structural stability.<sup>35,36</sup> We propose that catalase molecules engage in cooperative effect driven by specific self-interactions, which contribute to conformational stability by restricting excessive fluctuations and preventing loss of structural integration. Fig. 6(a) illustrates an isolated enzyme, while Fig. 6(b) depicts

an enzyme in a dense suspension. Although both systems share identical physical and chemical conditions, the presence of self-interactions in dense suspensions introduces an additional stabilization mechanism, preserving enzyme structure and function over extended periods.

We propose a possible explanation for the experimental results based on the unfolding behaviour of proteins. In Fig. 6(a), we illustrate the conformational changes of a single protein molecule in a dilute suspension, where intermolecular distances are large, and proteins behave independently. The loss of structural integrity can often be described as a two-step transition from the native to the denatured state. A key factor in determining protein stability is the difference in free energy between these two conformations. Since free energy consists of both enthalpic and entropic contributions, stabilization is influenced by changes in both. However, the relative contributions of these factors can vary depending on the specific protein and environmental conditions.

The enthalpy component of protein conformational changes arises from the disruption of intramolecular interactions such as hydrogen bonds, disulfide (S-S) bridges, and salt bridges, all of which contribute to the structural stability of the folded state. Breaking these stabilizing interactions requires energy and thus results in a positive enthalpic contribution (endothermic). At the same time, conformational changes may expose previously buried amino acid residues to the solvent, allowing new hydrogen bonds to form between the protein and surrounding water molecules, which introduces a negative enthalpic component (exothermic). While both effects are present, calorimetric studies on catalase<sup>37</sup> and similar proteins<sup>38</sup> suggest that the net enthalpy change associated with the loss of native protein structure is positive, indicating that the energetic cost of disrupting intramolecular bonds outweighs the favourable enthalpy of solvation. Therefore, the enthalpy is primarily

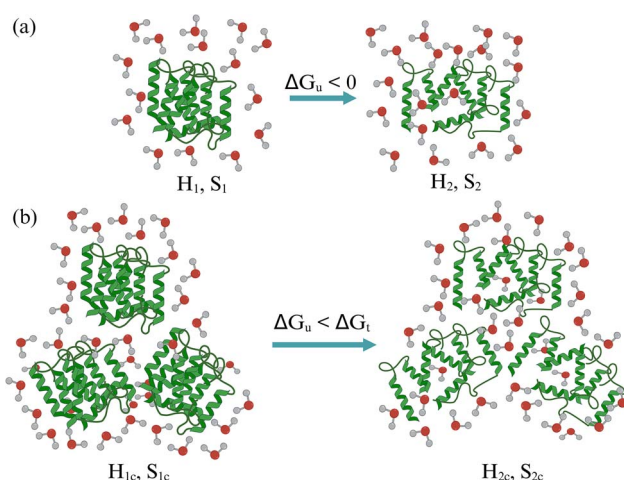


Fig. 6 Schematic illustration of enzyme stability in different suspensions: (a) denaturation and structural destabilization in a dilute suspension, and (b) enhanced stability and preserved conformation in a dense suspension due to self-interactions.



governed by the energy required to disrupt the folded structure. In the folded state, catalase is conformationally constrained. Upon being perturbed, it gains access to a vastly larger number of conformations, which increases the system's entropy. Additionally, while exposure of hydrophobic residues during the loss of native structure may cause water molecules to become more ordered (decreasing solvent entropy), this effect is usually outweighed by the large increase in protein conformational entropy. This is further supported by the calorimetric data available in the literature on catalase<sup>39</sup> and similar enzymes<sup>40</sup> that generally show positive  $\Delta S$  upon denaturation.

Let the enthalpy and entropy of the native and conformationally perturbed states be denoted as  $H_1$ ,  $H_2$ , and  $S_1$ ,  $S_2$  respectively. During conformational changes in catalase, these stabilizing interactions are disrupted, increasing the conformational entropy of the protein and also increasing the enthalpy.<sup>37,39</sup> The process is governed by the Gibbs free energy change:  $\Delta G_u = \Delta H_u - T\Delta S_u$ , where  $\Delta H_u = H_2 - H_1 > 0$  and  $\Delta S_u = S_2 - S_1 > 0$ , making  $\Delta G_u$  typically positive under native conditions. However, under elevated temperature or other denaturing conditions, the entropy gain can dominate, making the loss of catalase's native structure thermodynamically favourable.

Fig. 6(b) illustrates conformational perturbations in proteins in a dense suspension. Here, the intermolecular distance is reduced, leading to significant many-body interactions that alter the free energy landscape of protein unfolding. The total Gibbs free energy change for conformational changes can be written as,  $\Delta G_t = \Delta G_u + \Delta G_c$ , where  $\Delta G_c$  accounts for the additional effects arising from intermolecular interactions in a dense suspension. In dense suspensions, native proteins can form stabilizing contacts with each other *via* hydrogen bonds, salt bridges, hydrophobic patches or other long-range interactions. If conformational changes disrupt these interprotein interactions, and the newly exposed surfaces do not form equally strong compensatory contacts, the enthalpic cost of losing structural integrity increases ( $\Delta H_c > 0$ ). The conformational entropy may also decrease ( $\Delta S_c < 0$ ) due to spatial constraints and excluded volume effects.<sup>8,41,42</sup> Thus, the correction term due to many-body interactions  $\Delta G_c = \Delta H_c - T\Delta S_c$  can become positive. This additional stabilization term increases the total Gibbs free energy for unfolding ( $\Delta G_t > \Delta G_u$ ),

making the conformational changes less thermodynamically favourable in dense suspensions. The observed enhancement in enzyme stability can thus be attributed to cooperative interactions in dense suspensions, where proteins influence each other's conformational dynamics. This collective behaviour leads to a suppression of unfolding transitions, preserving both structural integrity and catalytic function over time.

A similar reduction in catalytic activity and conformational stability was observed in urease. To assess its activity, the decomposition of 10 mM urea was measured in the presence of 10 nM urease, taken from two different stock solutions: 10 nM and 10  $\mu$ M. As shown in Fig. 7(a), urease activity decreased over time, but the decline is significantly slower in the dense suspension compared to that in the dilute one, indicating enhanced stability. Fig. 7(b) further supports this observation, showing a time-dependent reduction in fluorescence intensity, which is more pronounced in the dilute suspension – suggesting that the conformational stability of urease is better preserved in dense suspensions.

We finally investigated whether active mechanical fluctuations generated by localized enzyme catalysis in fluidic environments influence enzyme stability. Recent studies suggest that such fluctuations, even in dense and crowded conditions, can significantly alter the dynamics of their surroundings.<sup>43–46</sup> While the precise mechanism underlying the dynamic coupling between active enzymes and their immediate environment remains unclear, enzymes have been proposed to interact mechanically with their surroundings *via* both long-range hydrodynamic interactions<sup>47–49</sup> and high-frequency pressure waves.<sup>50,51</sup> The hydrodynamic interactions are known to play a crucial role in macromolecular association and mobility.<sup>52</sup> Recent findings indicate that enzymatic activity can be modulated through hydrodynamic interactions driven fluctuations,<sup>34</sup> although the extent to which these interactions affect protein folding remains a subject of debate.<sup>53,54</sup> Several studies support the idea that solvent flow-induced hydrodynamic interactions dynamically couple amino acid residues, thereby influencing folding pathways.<sup>55–59</sup> Notably, computational studies employing the fluid particle dynamics method suggest that hydrodynamic interactions promote fast-folding pathways. This accelerates the attainment of the native state, minimizes kinetic

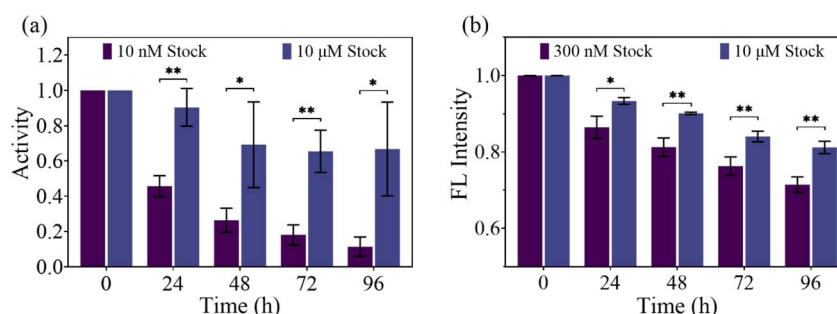
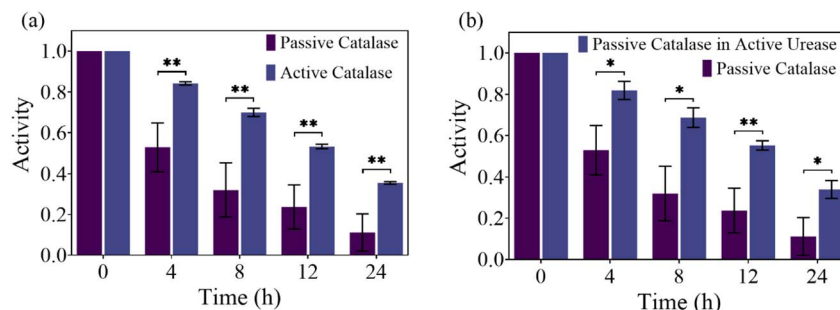


Fig. 7 (a) Time-dependent reduction in urease catalytic activity measured for 10 nM urease in the presence of 10 mM urea, with enzymes taken from stock solutions of 10 nM and 10  $\mu$ M. Data were normalized with respect to the catalytic activity measured at time  $t = 0$  h. (b) Fluorescence intensity decay of 300 nM urease over time, comparing samples taken from two different stock solutions: 300 nM and 10  $\mu$ M. Data were normalized with respect to the fluorescence intensity measured at time  $t = 0$  h.





**Fig. 8** (a) Time-dependent decay of catalytic activity of 1 nM catalase preserved in normal aqueous environment (passive catalase) and in an actively fluctuating environment (active catalase), generated by catalase itself. (b) Time-dependent decay of catalytic activity of 1 nM catalase preserved in a normal aqueous environment (passive catalase) and an actively fluctuating environment (passive catalase in active urease), generated by the urea–urease reaction. Data were normalized with respect to the catalytic activity measured at time  $t = 0$  h.

trapping, and significantly enhances folding kinetics compared to scenarios without such interactions.<sup>60</sup>

The generation of acoustic pulses during catalytic reactions may also contribute to conformational stability in dense enzyme suspensions by limiting domain fluctuations.<sup>61</sup> It could further be inferred from the concept of swim pressure, which is believed to arise from the autonomous propulsion of catalytic micromotors in fluidic media.<sup>62</sup> These interactions could potentially exert mechanical effects on neighbouring molecules, thereby influencing their conformation in active environments.

To explore this experimentally, we studied the stability of 1 nM catalase in the presence and absence of its substrate (a continuous flow of 10 mM H<sub>2</sub>O<sub>2</sub>). Fig. 8(a) presents the time-dependent decay of catalytic activity with and without active fluctuations. Notably, catalase retains its activity for a longer duration in the presence of activity, suggesting that enzyme-driven fluctuations help stabilize protein conformation. To test the non-specificity of active fluctuations, the experiments were repeated with molecules of urease as a source of active forces (10 nM urease, with continuous supply of 100 mM urea). In the presence of urease activity, we studied the catalytic stability of 1 nM catalase by measuring the reaction rate at different preservation times and compared it with that of the passive suspension case as shown in Fig. 8(b). Here we observed that the catalytic activity of catalase decayed slowly compared to the passive suspension. In both cases, catalytic stability of 1 nM catalase was studied by measuring the decomposition rate of 10 mM H<sub>2</sub>O<sub>2</sub> in the presence of 1 nM catalase at different preservation times (0 h, 4 h, 8 h, 12 h, 24 h). Before measuring substrate decomposition, we confirmed that the supplied substrate did not contribute to catalytic activity by measuring the absorbance at 240 nm of 1 nM catalase taken from the active stock suspension, which showed a value close to zero.

Thus, for both active catalase and active urease suspensions, fluctuations generated during substrate catalysis appear to help preserve the catalytic activity of catalase enzyme over extended periods. As a result, the catalytic activity decays more slowly over time in the active samples than in the passive ones. This preservation of catalytic activity is likely due to the preserved native conformation of catalase in the active suspensions. The fluctuations generated by the active enzyme may exert mechanical

pressure on the surfaces of the neighbour enzymes.<sup>50</sup> Additionally, the motion of active enzymes may generate swim pressure on nearby molecules,<sup>62</sup> potentially stabilizing their conformations. These results are particularly interesting because they contrast with typical active matter systems, where active fluctuations generally enhance mobility and raise the effective temperature of the system. In our study, however, active fluctuations appear to help preserve the conformation of catalase, thereby producing a cooling-like effect.

## Conclusion

Our study demonstrates that the stability and catalytic activity of enzymes in aqueous environments are strongly influenced by intermolecular interactions and active mechanical fluctuations. In dilute suspensions, proteins undergo conformational destabilization due to enhanced entropy in the unfolded state, leading to a time-dependent loss of catalytic function. However, at higher concentrations, many-body interactions and collective effects contribute to stabilizing protein conformation by increasing enthalpic contributions and reducing conformational entropy in the unfolded state. Furthermore, our results suggest that catalytic activity may help preserve enzymatic function over extended periods, potentially through the generation of active mechanical stress that originates near the catalytic sites and influences the surrounding environment. While our findings are consistent with this hypothesis, direct measurements of such fluctuations, as well as insights into their mode of propagation around enzymes, will be important in future studies to confirm their role in structural stabilization.

## Experimental

### Materials

Catalase from bovine liver (catalogue no: C9322), urease from *Canavalia ensiformis* (Jack bean, catalogue no: U1500), urea (catalogue no: U5128), phenol red (catalogue no: P3532), glycerol (catalogue no: G5516), Ficoll PM 400 (catalogue no: F4375), Ficoll PM 70 (catalogue no: F2878), and dextran 70 from *Leuconostoc* spp. (catalogue no: 31390) were purchased from Sigma-Aldrich. A 30% (w/v) hydrogen peroxide (H<sub>2</sub>O<sub>2</sub>) solution



(catalogue no: 107209) was obtained from Merck. Bovine Serum Albumin (BSA) (CAS: 9048-46-8) was purchased from SRL, India.

### UV-vis spectroscopy study

The kinetics of  $\text{H}_2\text{O}_2$  decomposition in the presence of catalase was monitored by measuring its absorbance at 240 nm over time. The reaction was conducted for 2 min, after which absorbance *versus* time data were plotted and fitted with a linear regression model to determine the catalytic activity of catalase. Similarly, the kinetics of urea decomposition in the presence of urease was studied by measuring the absorbance of phenol red at 560 nm over time. After 5 min of reaction, absorbance *versus* time data were plotted, and the urease activity was quantified by calculating the area under the curves.

### Fluorescence spectroscopy study

The aromatic residues such as tryptophan and tyrosine within the enzyme structure contribute to its intrinsic fluorescence. Changes in the local environment of these residues lead to fluorescence quenching, making fluorescence intensity a useful indicator of protein conformational stability. Fluorescence measurements were carried out with an excitation wavelength of 280 nm, emission spectra were recorded from 320 nm to 355 nm wavelength range, and the emission intensity were measured at 336 nm.

### Circular dichroism (CD) spectroscopy study

CD spectra were recorded in the wavelength range of 190–250 nm to analyze secondary structural changes. A minimum at 208 nm corresponded to  $\alpha$ -helix absorption, while a minimum at 215 nm indicated  $\beta$ -sheet absorption. The  $\alpha$ -helix content was calculated from the CD spectra using the ellipticity value at 208 nm.<sup>20,23</sup>

### Generation of active fluctuations

**Active catalase.** In 1 nM catalase suspension, 10 mM  $\text{H}_2\text{O}_2$  was supplied continuously through a syringe pump. The initial volume of the suspension was 40 mL and the rate of substrate flow was maintained at 100  $\mu\text{L h}^{-1}$ . The kinetics study was carried out at 0 h, 4 h, 8 h, 12 h, and 24 h of preservation. After 8 h, the stock volume was reduced to 20 mL and the substrate flow rate was maintained at 50  $\mu\text{L h}^{-1}$ .

**Passive catalase in active urease suspension.** Aqueous suspensions of catalase and urease were mixed to obtain a final stock containing 1 nM catalase and 10 nM urease. 100 mM urea was supplied continuously through a syringe pump. The initial volume of the suspension was 40 mL and the rate of substrate flow was maintained at 100  $\mu\text{L h}^{-1}$ . The kinetics study was carried out at 0 h, 4 h, 8 h, 12 h, and 24 h of preservation. After 8 h, the stock volume was reduced to 20 mL and the substrate flow rate was maintained at 50  $\mu\text{L h}^{-1}$ .

### Error estimation and statistical significance

Each experiment was performed three times, and the mean values of the measured parameters are reported. Error bars

represent the standard deviation of the measurements. Statistical significance was assessed using Student's *t*-test, with  $p < 0.05$  considered significant. The symbols \*, \*\*, \*\*\*, and \*\*\*\* represent  $p < 0.05$ ,  $p < 0.01$ ,  $p < 0.001$ , and  $p < 0.0001$ , respectively. The notation 'ns' indicates not significant.

### Conflicts of interest

The authors declare no conflict of interest.

### Data availability

Data for this article are available at Science Data Bank <https://www.scidb.cn/en/s/MNvYBb> at <https://doi.org/10.57760/sciencedb.24267>.

### Acknowledgements

KKD thanks Anusandhan National Research Foundation (ANRF), India (CRG/2023/007588, CRD/2024/000753), Ministry of Education, Government of India (MoE-STARS/STARS-2/2023-0620), Gujarat State Biotechnology Mission (GSBTM/RSS/E-FILE/30/2024/0021/04952485) and IIT Gandhinagar for financial support. Helpful discussions with Dr Mithun Radhakrishna, Dr Ashutosh Srivastava, and Dr Dhiraj Bhatia are gratefully acknowledged. We thank the Center for Research & Development of Scientific Instruments (CRDSI), IIT Jodhpur, for providing access to the Circular Dichroism facility.

### References

- 1 C. ÓFágáin, *Enzyme Microb. Technol.*, 2003, **33**, 137–149.
- 2 C. Mateo, J. M. Palomo, G. Fernandez-Lorente, J. M. Guisan and R. Fernandez-Lafuente, *Enzyme Microb. Technol.*, 2007, **40**, 1451–1463.
- 3 V. V. Mozhaev, N. S. Melik-Nubarov, M. V. Sergeeva, V. Šikšnis and K. Martinek, *Biocatal.*, 1990, **3**, 179–187.
- 4 C. P. Govardhan, *Curr. Opin. Biotechnol.*, 1999, **10**, 331–335.
- 5 E.-H. Lee, T. Tsujimoto, H. Uyama, M.-H. Sung, K. Kim and S. Kuramitsu, *Polym. J.*, 2010, **42**, 818–822.
- 6 K. Luby-Phelps, *Int. Rev. Cytol.*, 1999, **192**, 189–221.
- 7 H.-X. Zhou, G. Rivas and A. P. Minton, *Annu. Rev. Biophys.*, 2008, **37**, 375–397.
- 8 M. Senske, L. Törk, B. Born, M. Havenith, C. Herrmann and S. Ebbinghaus, *J. Am. Chem. Soc.*, 2014, **136**, 9036–9041.
- 9 A. C. Miklos, M. Sarkar, Y. Wang and G. J. Pielak, *J. Am. Chem. Soc.*, 2011, **133**, 7116–7120.
- 10 T. Vöpel and G. I. Makhatadze, *PLoS One*, 2012, **7**, e39418.
- 11 I. Pozdnyakova and P. Wittung-Stafshede, *Biochim. Biophys. Acta*, 2010, **1804**, 740–744.
- 12 V. Nolan, A. Collin, C. Rodriguez and M. A. Perillo, *J. Agric. Food Chem.*, 2020, **68**, 8875–8882.
- 13 B. K. Derham and J. J. Harding, *Biochim. Biophys. Acta*, 2006, **1764**, 1000–1006.
- 14 C. Bollen, L. Dewachter and J. Michiels, *Front. Mol. Biosci.*, 2021, **8**, 669664.
- 15 T. Ooi and M. Oobatake, *J. Biochem.*, 1988, **103**, 114–120.



16 H. S. Muddana, S. Sengupta, T. E. Mallouk, A. Sen and P. J. Butler, *J. Am. Chem. Soc.*, 2010, **132**, 2110–2111.

17 S. Sengupta, K. K. Dey, H. S. Muddana, T. Tabouillot, M. E. Ibele, P. J. Butler and A. Sen, *J. Am. Chem. Soc.*, 2013, **135**, 1406–1414.

18 A.-Y. Jee, Y.-K. Cho, S. Granick and T. Tlusty, *Proc. Natl. Acad. Sci. U. S. A.*, 2018, **115**, E10812–E10821.

19 A.-Y. Jee, T. Tlusty and S. Granick, *Proc. Natl. Acad. Sci. U. S. A.*, 2020, **117**, 29435–29441.

20 D. Majumder, A. Das and C. Saha, *Int. J. Biol. Macromol.*, 2017, **104**, 929–935.

21 M.-C. Bellissent-Funel, A. Hassanali, M. Havenith, R. Henchman, P. Pohl, F. Sterpone, D. v. d. Spoel, Y. Xu and A. E. Garcia, *Chem. Rev.*, 2016, **116**, 7673–7697.

22 Y. Levy and J. N. Onuchic, *Proc. Natl. Acad. Sci. U. S. A.*, 2004, **101**, 3325–3326.

23 Y. Wei, A. A. Thyparambil and R. A. Latour, *Biochim. Biophys. Acta*, 2014, **1844**, 2331–2337.

24 V. La Verde, P. Dominici and A. Astegno, *Bio-Protoc.*, 2017, **7**, e2230.

25 V. T. Ranganathan, S. Bazmi, S. Wallin, Y. Liu and A. Yethiraj, *Macromolecules*, 2022, **55**, 9103–9112.

26 J. K. Armstrong, R. B. Wenby, H. J. Meiselman and T. C. Fisher, *Biophys. J.*, 2004, **87**, 4259–4270.

27 C. Follmer, F. V. Pereira, N. P. da Silveira and C. R. Carlini, *Biophys. Chem.*, 2004, **111**, 79–87.

28 F. L. G. Flecha and V. Levi, *Biochem. Mol. Biol. Educ.*, 2003, **31**, 319–322.

29 A. Charkhesht, D. Lou, B. Sindle, C. Wen, S. Cheng and N. Q. Vinh, *J. Phys. Chem. B*, 2019, **123**, 8791–8799.

30 K. Nasreen, Z. A. Parray, S. Ahamad, F. Ahmad, A. Ahmed, S. F. Alamery, T. Hussain, Md. I. Hassan and A. Islam, *Biomolecules*, 2020, **10**, 490.

31 W. Gtari, H. Bey, A. Aschi, L. Bitri and T. Othman, *Mater. Sci. Eng. C*, 2017, **72**, 98–105.

32 Y. Liu, E. Fratini, P. Baglioni, W.-R. Chen and S.-H. Chen, *Phys. Rev. Lett.*, 2005, **95**, 118102.

33 M. M. Gromiha and S. Selvaraj, *Biophys. Chem.*, 1999, **77**, 49–68.

34 A. K. Tripathi, T. Das, G. Paneru, H. K. Pak and T. Tlusty, *Commun. Phys.*, 2022, **5**, 101.

35 S. von Bülow, M. Siggel, M. Linke and G. Hummer, *Proc. Natl. Acad. Sci. U. S. A.*, 2019, **116**, 9843–9852.

36 M. Grimaldo, F. Roosen-Runge, F. Zhang, F. Schreiber and T. Seydel, *Q. Rev. Biophys.*, 2019, **52**, 1–63.

37 E. Blanco, J. M. Russo, J. Sabin, G. Prieto and F. Sarmiento, *J. Therm. Anal. Calorim.*, 2007, **87**, 143–147.

38 G. R. Behbehani, A. A. Saboury and E. Taleshi, *Colloids Surf. B*, 2008, **61**, 224–228.

39 G. Prieto, M. J. Suárez, A. González-Pérez, J. M. Russo and F. Sarmiento, *Phys. Chem. Chem. Phys.*, 2004, **6**, 816–821.

40 J. Seelig and A. Seelig, *Biophys. Rep.*, 2022, **2**, 100037.

41 S. Mo, X. Shao, Y. Chen and Z. Cheng, *Sci. Rep.*, 2016, **6**, 36836.

42 B. C. Rocha, S. Paul and H. Vashisth, *Entropy*, 2020, **22**, 877.

43 X. Zhao, K. K. Dey, S. Jeganathan, P. J. Butler, U. M. Córdova-Figueroa and A. Sen, *Nano Lett.*, 2017, **17**, 4807–4812.

44 A. Maiti, Y. Koyano, H. Kitahata and K. K. Dey, *Phys. Rev. E*, 2024, **109**, 054607.

45 X. Lin and Y. He, *Anal. Chem.*, 2022, **94**, 7158–7163.

46 Nividha, A. Maiti, K. Parihar, R. Chakraborty, P. Agarwala, D. K. Sasmal, R. Radhakrishnan, D. Bhatia, and K. K. Dey, *bioRxiv*, 2024, preprint, DOI: [10.1101/2024.12.05.627033](https://doi.org/10.1101/2024.12.05.627033).

47 A. S. Mikhailov and R. Kapral, *Proc. Natl. Acad. Sci. U. S. A.*, 2015, **112**, E3639–E3644.

48 R. Kapral and A. S. Mikhailov, *Physica D*, 2016, **318–319**, 100–104.

49 Y. Koyano, H. Kitahata and A. S. Mikhailov, *Europhys. Lett.*, 2019, **128**, 40003.

50 R. Chakraborty, A. Maiti, D. Paul, R. Borthakur, K. R. Jayaprakash, U. Ghosh, and K. K. Dey, *arXiv*, 2024, preprint, arXiv:2408.00578, DOI: [10.48550/arXiv.2408.00578](https://doi.org/10.48550/arXiv.2408.00578).

51 C. Riedel, R. Gabizon, C. A. M. Wilson, K. Hamadani, K. Tsekouras, S. Marqusee, S. Pressé and C. Bustamante, *Nature*, 2015, **517**, 227–230.

52 T. Ando and J. Skolnick, *Proc. Natl. Acad. Sci. U. S. A.*, 2010, **107**, 18457–18462.

53 F. C. Zegarra, D. Homouz, Y. Eliaz, A. G. Gasic and M. S. Cheung, *Phys. Rev. E*, 2018, **97**, 032402.

54 N. Kikuchi, J. F. Ryder, C. M. Pooley and J. M. Yeomans, *Phys. Rev. E*, 2005, **71**, 061804.

55 A. Baumketner and Y. Hiwatari, *J. Phys. Soc. Jpn.*, 2002, **71**, 3069–3079.

56 H. Tanaka, *J. Phys.: Condens. Matter*, 2005, **17**, S2795–S2803.

57 P. Szymczak and M. Cieplak, *J. Phys.: Condens. Matter*, 2011, **23**, 033102.

58 M. Cieplak and S. Niewieczorzał, *J. Chem. Phys.*, 2009, **130**, 124906.

59 T. Frembgen-Kesner and A. H. Elcock, *J. Chem. Theory Comput.*, 2009, **5**, 242–256.

60 J. Yuan and H. Tanaka, *Phys. Rev. Lett.*, 2024, **132**, 138402.

61 M. Souza, E. T. Mezadri, E. Zimmerman, E. X. Leaes, M. M. Bassaco, V. D. Prá, E. Foletto, A. Cancellier, L. M. Terra, S. L. Jahn and M. A. Mazutti, *Ultrason. Sonochem.*, 2013, **20**, 89–94.

62 S. C. Takatori, W. Yan and J. F. Brady, *Phys. Rev. Lett.*, 2014, **113**, 028103.

